

Optical tomography of phase objects with parallel projection differences and ESPI

C. Meneses-Fabian, G. Rodríguez-Zurita, and J.F. Vázquez-Castillo

*Benemérita Universidad Autónoma de Puebla, Facultad de Ciencias Físico-Matemáticas
Ciudad Universitaria, San Manuel
C.P. 72570, Puebla, Pue., MEXICO.*

Recibido el 18 de octubre de 2002; aceptado el 21 de enero de 2003

This paper describes a technique that obtains border-enhanced tomographic images of a slice belonging to a phase object. This is obtained experimentally by means of the sequential storage of differences of parallel projections from two adjacent angular positions of the object and with appropriate techniques for their reconstruction. An ESPI (Electronic Speckle Pattern Interferometry) system is used in a Mach-Zehnder configuration to obtain data. Computer simulations are shown as well as experimental results.

Keywords: Tomography; speckle; interferometry; phase shifting; image reconstruction.

Se describe un método para obtener una imagen tomográfica con bordes realzados perteneciente a una rebanada de un objeto de fase. Experimentalmente, el realce se obtiene mediante el almacenamiento secuencial de las diferencias de distribución de índice de refracción a dos posiciones angulares adyacentes del objeto y con técnicas apropiadas para su reconstrucción. Se emplea un sistema ESPI (interferómetro electrónico de patrones de moteado) en configuración Mach-Zehnder para la obtención de los datos. Se muestran simulaciones a computadora y resultados experimentales.

Descriptores: Tomografía; speckle; interferometría; muestreo de fase; reconstrucción de imágenes.

PACS: 42.30.Wb; 42.30.Ms; 42.30.Rx; 42.87.Bg

1. Introduction

It has been proposed the use of parallel projections in tomographic reconstruction to enhance tomographic image borders [1, 2]. Such differences can be experimentally measured with the use of a proper storage system [?]. They provide the possibility to overcome some limitations in measurement range due to a fixed reference. ESPI (Electronic Speckle Pattern Interferometry) [?] is a candidate to develop a difference system because it performs storage properly. In this work, a description of an experimental ESPI system to reconstruct enhanced images of transparent objects is given. Computer simulations and experimental results are also discussed.

2. Tomography with parallel projection differences

2.1. Angular derivative of parallel projections

The proposed tomographic method with parallel projections differences is illustrated in Fig. 1 using a rectangular refractive index slice distribution $f(x, y)$ (of constant value within a rectangle, first row) as an example. Two sinograms (denoted by $\check{f}_\phi(p)$ and $\check{f}_{\phi+\Delta\phi}(p)$) obtained from the same refractive index slice $f(x, y)$ are shown in the second row. Each one is calculated at two slightly different projecting angles ϕ and $\phi + \Delta\phi$, with $\Delta\phi = 5^\circ$. Thus, they are mutually displaced by a constant angle of 5° along the ϕ -axis. Their

subtraction,

$$\Delta\check{f}_\phi(p) = \check{f}_{\phi+\Delta\phi}(p) - \check{f}_\phi(p), \quad (1)$$

is shown in the third row (both as a gray-level plot and as a 3-D graph) and is an approximation to the angular derivative of the projections, *i.e.*,

$$\frac{\partial}{\partial\phi}\check{f}_\phi(p) = \frac{\partial}{\partial\phi}\Re_\phi\{f(x, y)\}, \quad (2)$$

where

$$\begin{aligned} \check{f}_\phi(p) &= \Re_\phi\{f(x, y)\} \\ &= \int_{-\infty}^{+\infty} \int_{-\infty}^{+\infty} f(x, y) \delta(p - x \cos \phi - y \sin \phi) dx dy \quad (3) \end{aligned}$$

denotes the Radon transform of $f(x, y)$ at angle ϕ [2, 4]. Backprojection of filtered differences of projections shows edge enhancement of the original slice distribution (fourth row). Such an image coincides with the subtraction of the backprojection of the individual filtered projections, shown in the same Fig. 1 (bottom, fifth row).

2.2. Radon transform of angular derivative

The angular derivative of a parallel projection can be further written as [1, 2]

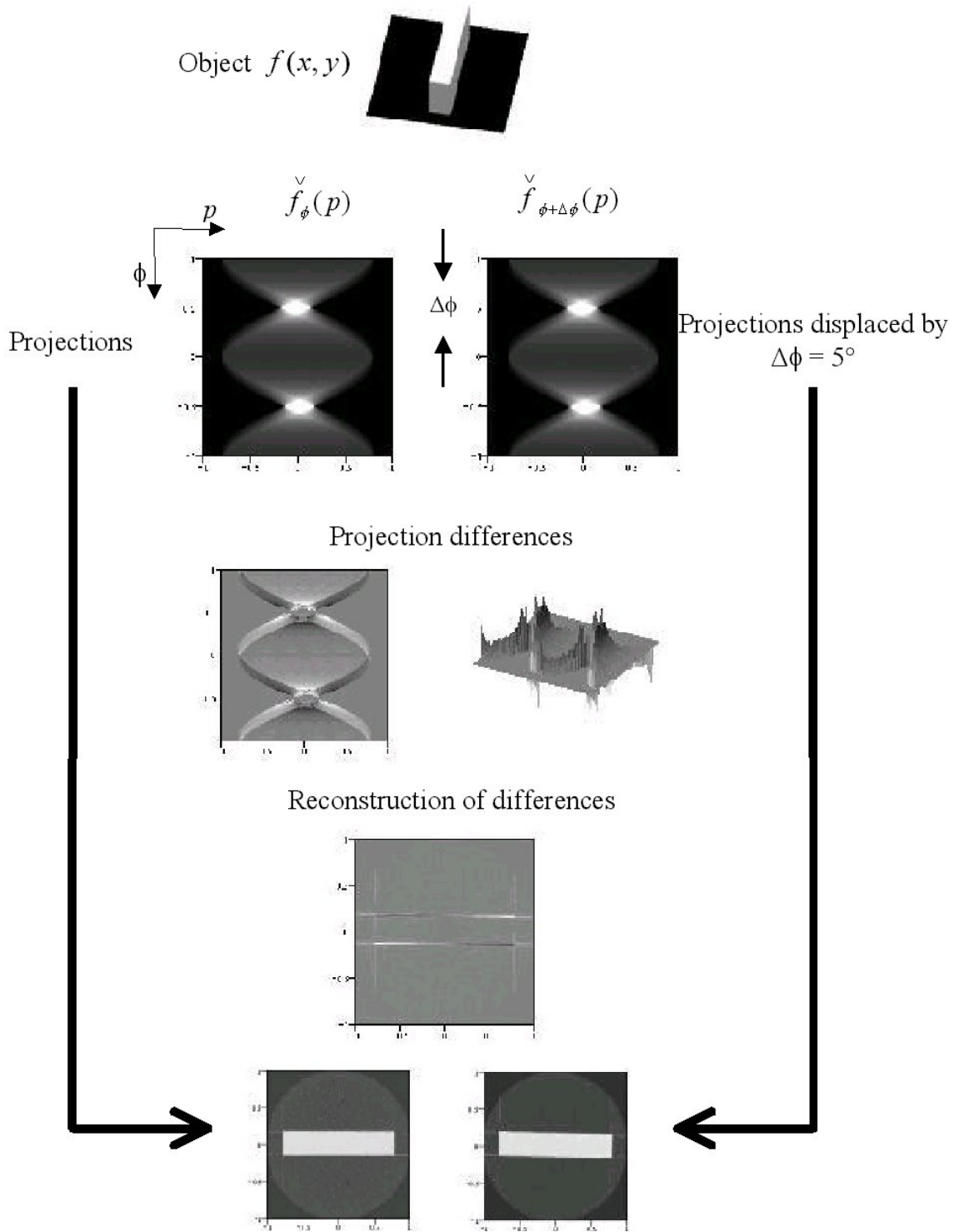


FIGURE 1. Parallel projection differences.

$$\frac{\partial}{\partial \phi} \mathfrak{R}_\phi \{f(x, y)\} = \int_{-\infty}^{+\infty} dx \int_{-\infty}^{+\infty} dy \left\{ f(x, y) \frac{\partial}{\partial \phi} \delta(p - x \cos \phi - y \sin \phi) + \delta(p - x \cos \phi - y \sin \phi) \frac{\partial}{\partial \phi} f(x, y) \right\}, \quad (4)$$

but, for points belonging to the line $(x, p \csc \phi - x \cot \phi)$ and with $u = p - x \cos \phi - y \sin \phi$,

$$\begin{aligned} \frac{\partial}{\partial \phi} \delta(p - x \cos \phi - y \sin \phi) &= -\frac{\partial}{\partial u} \delta(u) \left(x \frac{\partial}{\partial \phi} \cos \phi + y \frac{\partial}{\partial \phi} \sin \phi + \frac{\partial}{\partial \phi} \cos \phi \frac{\partial x}{\partial \phi} + \sin \phi \frac{\partial y}{\partial \phi} \right) \\ &= -\frac{\partial}{\partial u} \delta(u) [-x \sin \phi + (p \csc \phi - x \cot \phi) \cos \phi - p \cot \phi + x \csc \phi] = 0, \end{aligned}$$

thus, according to Eq. (4), this gives the result

$$\frac{\partial}{\partial \phi} \mathfrak{R}_\phi \{f(x, y)\} = \mathfrak{R}_\phi \left\{ \frac{\partial}{\partial \phi} f(x, y) \right\}. \quad (5)$$

Then, the Radon transform of the angular derivative of the slice equals the angular derivative of the Radon transform, which gives insight of the edge enhancement found in the example of Fig. 2. It is a reconstruction of the angular derivative of the slide.

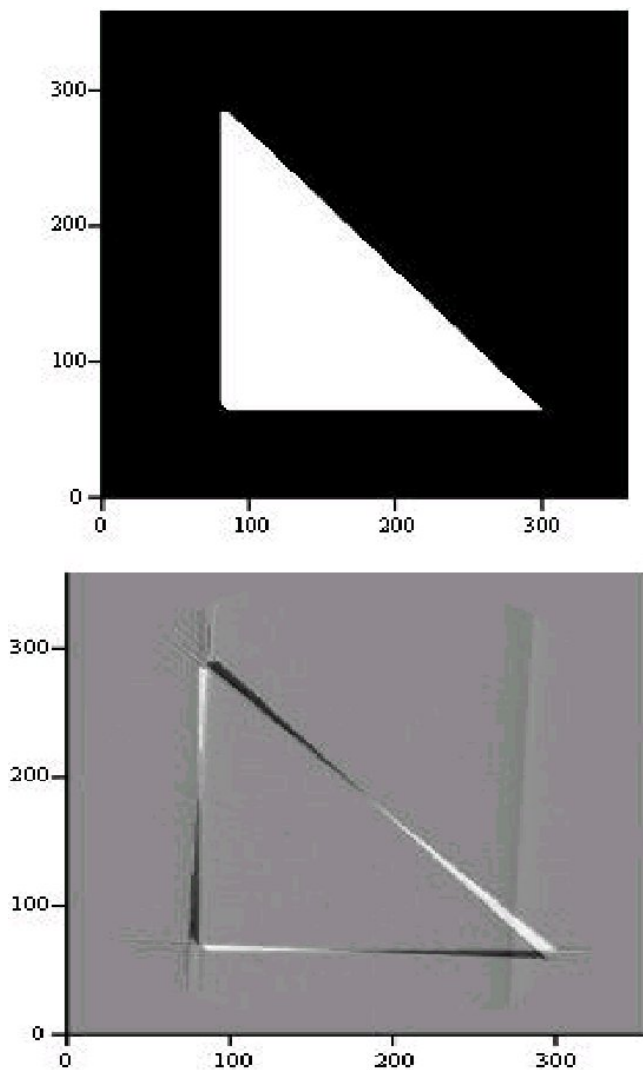


FIGURE 2. Parallel projection reconstruction (right) of a triangle (left). 360x360 pixels.

Another slice is also simulated in Fig. 2 (a triangle, above) as well as the reconstruction of differences (below, $\Delta \phi = 2^\circ$). Note the changes above and below the average level.

2.3. Experimental difference extraction.

Assuming the refractionless case, a projection at angle ϕ is a phase object of the form

$$\exp \left[i \left(\frac{2\pi}{\lambda} \right) \check{f}_\phi(p) \right]. \quad (6)$$

When performing the superposition of two adjacent projections, an interference pattern $I_\phi(p)$ of the form [1, 4]

$$I_\phi(p) = 2 \left\{ 1 + \cos \left[\frac{2\pi}{\lambda} (\check{f}_{\phi+\Delta\phi}(p) - \check{f}_\phi(p)) \right] \right\}, \quad (7)$$

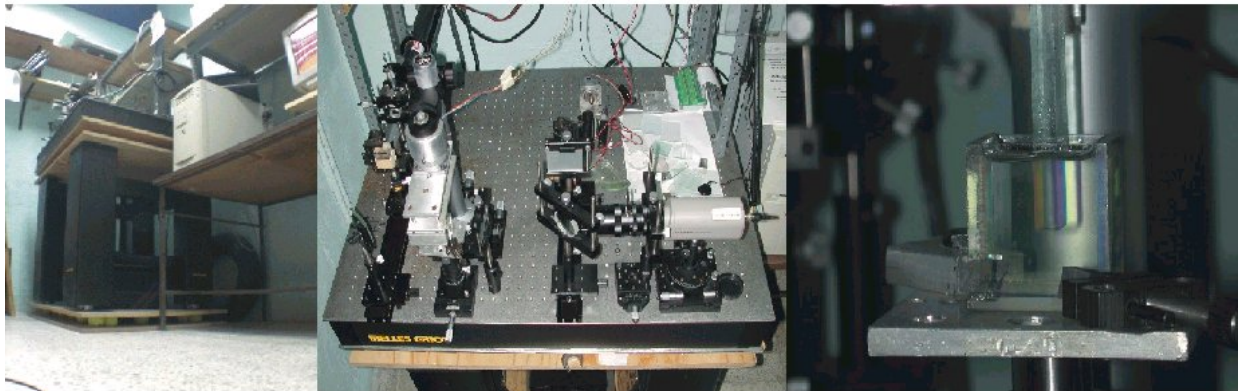
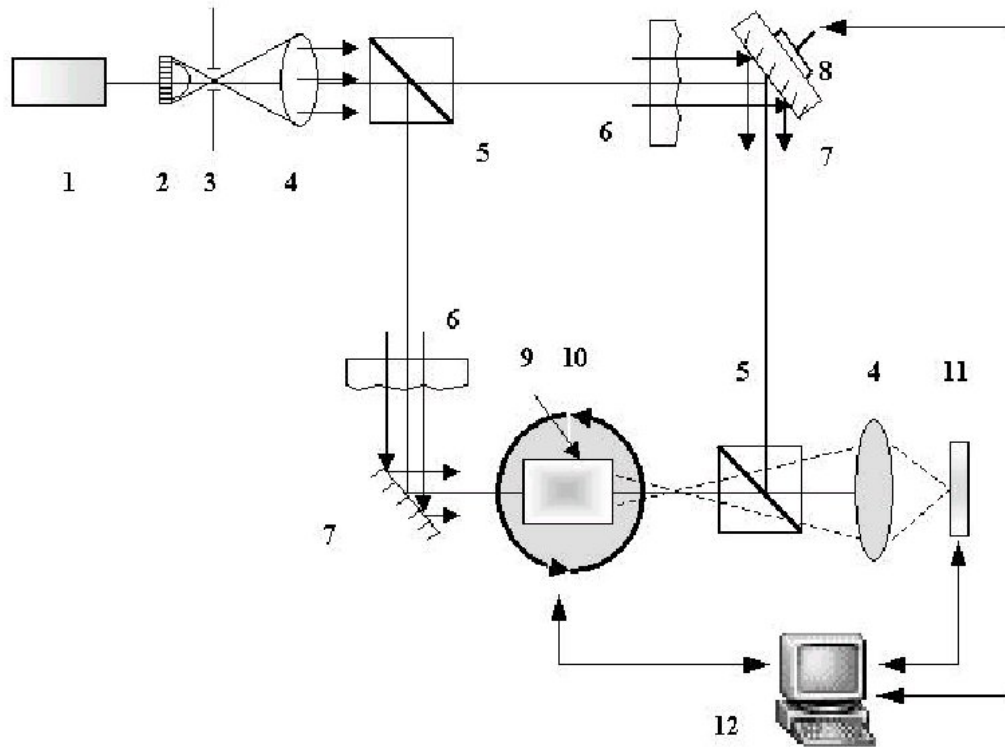
results. Then, $\Delta \check{f}_\phi(p)$ of Eq.(1) can be extracted with interferometric methods. To carry out such a superposition, appropriate storage of at least one projection is required.

Among others, ESPI (Electronic Speckle Pattern Interferometry) is a possible technique able to render experimentally difference of phase projections because it contains the required image storage of projection at angle ϕ (speckle pattern), while the projection at angle $\phi + \Delta\phi$ can be extracted from the real-time speckle pattern [3, 5]. Absolute value of subtraction can be attained with this technique. Phase-stepping techniques can also be incorporated to calculate wrapped phase. With this method, it is expected to get images related with the angular derivative of phase slices.

3. Experimental set-up

3.1. ESPI set-up

Figure 3 shows the experimental set-up, which basically consists of a Mach-Zehnder interferometer with a piezoelectrically driven mirror in the reference arm (7, 8). Scattering plates (6) help to speckle formation. A glass sample (immersed in a fixed liquid gate) is placed in the other arm and is rotated by a stepping motor (10) driven by a computer (12). Image of the exit plane is formed by lens (4) on the CCD (11). Photographs of some details are also shown.



Setup in laboratory (1-12)

Setup (1-11)

sample in liquid-gate (9)

FIGURE 3. Experimental set-up (ESPI). 1. Laser, 2. Microscope objetive, 3. Pinhole, 4. Lenses, 5. Cube beam splitters, 6. Scatter plates, 7. Mirrors, 8. Piezo driver (PZT), 9. Sample & liquid gate, 10. Stepping motor, 11. CCD, 12. Computer.

3.2. Phase matching test (condition for parallel projections)

Figure 4 shows three interferograms of a plane-parallel glass plate immersed in the liquid gate as seen through the CCD. Interference results between two adjacent projections. The patterns are watched at the computer monitor as a result of speckle pattern subtraction. Each interferogram appears due to phase shifting in the reference arm. The entire field results

divided by the plate borders (three thin dark lines) and a pair of bright parallel lines formed by two caustics (middle of the field). The central region between bright lines shows practically only one interference fringe, indicating a near constant phase distribution. The two side regions shows nearly parallel fringes suggesting a linear phase variation.

This observation can be explained in terms of Fig. 5, which shows some parallel projections of a rectangular slice with constant refractive index. The two rays passing through

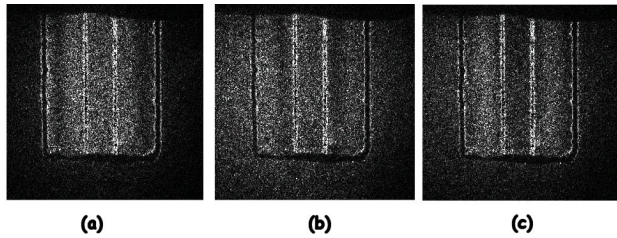


FIGURE 4. ESPI interferograms of a plate in three different phase shifts.

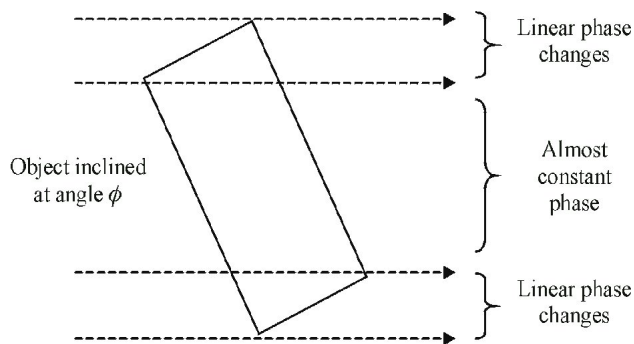


FIGURE 5. Parallel rays crossing through a rectangular section without refraction.

the plate but crossing a plate's inner corner define an area with a constant optical path in between. This region corresponds itself to the area between bright lines in Fig. 4. From each of the above mentioned rays to the ones touching the outermost plate's corners, the optical paths decrease linearly. These are the two areas of parallel fringes of Fig. 4. The result is interpreted as a consequence of approaching the refractionless condition.

4. Experimental results for optical tomography with ESPI

Some typical experimental results from the system as described are shown. The sample is rotated within the angular range from 0° to 180° . Projections for the range 180° to 360° are obtained by using the symmetries of Radon transforms as usual. Angular step was of 0.91° . Oil refractive index was 1.515.

Example 1. Glass plate

The sinogram of one of the preliminary results is shown at left of Fig. 6. There are some information to be recognized in the sinogram. However, discontinuities along ϕ and p directions are to be seen. They arise mainly from to the phase-unwrapping algorithm, which gives rise to arbitrary phase levels of piecewise constant values. On one side, there are no relation between projection differences of different projecting angles, which accounts for discontinuities along the ϕ -axis. On the other side, projection differences show points

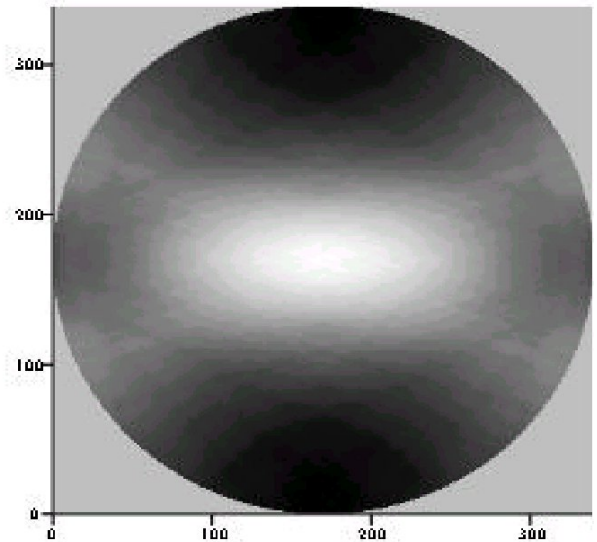
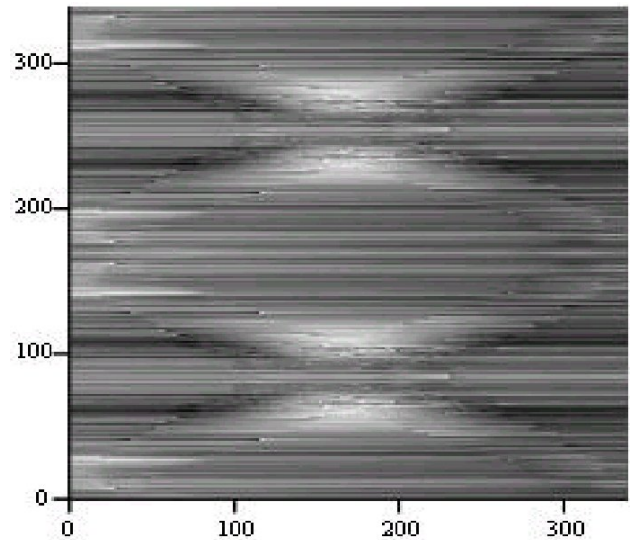


FIGURE 6. Sinogram of the rectangular object and its reconstruction.

of discontinuities, so unwrapping of one and the same projection at a given projecting angle gives values with certainty up to a constant. This gives discontinuities along p -axis.

At the right of Fig. 6, a reconstruction by backprojection of filtered projections is also shown. Although some rectangular distribution can be retrieved, no edge enhancement could be detected.

Example 2. Glass bar with square section

A glass bar with nearly squared cross section was used as another test object. This time, the sinogram was subject to some process before reconstruction. Taking into account the two main sources for discontinuities as described, identification of segments of constant phase was first carried out with the help of simulated projections. One of such segments were

the ones corresponding to the projection values outside of the object boundaries, which have to be of zero value. Choosing one side, say, the left side, for a given projection difference, the average value corresponding to that segment was subtracted from each experimental data of the same segment. The same procedure was applied to the right side segments. This procedure did eliminate discontinuities outside the object, as the plots of the Fig. 7a show. Then, the procedure lives inspection of only the central part. No further changes were done because no high discrepancies with simulations were detected. Linear interpolation was also performed to fill the range where measurements were not possible due to high frequency in the resulting interference fringes (between 80° and 100°). Resulting reconstructions can be seen in Fig. 7b, c y d. Edge enhancement is now to be recognized. High intensity is displayed at the square corners. At the bottom line, absolute value of reconstruction is displayed.

Example 3. Testing tube (out of centre)

As another sample, a testing tube was inspected. The tube's symmetry center was placed in no coincidence with the rotation center. Processing similar to the previous case was carried out for the sinogram. Reconstruction effectively displays both outer and inner border sides, as well as its position, which is revealed to be out of centering (Fig. 8). Due to the relative low values of differences, noise is to be noticeable. For visual inspection purposes, however, simple techniques to minimize this effect (as thresholding) can be applied.

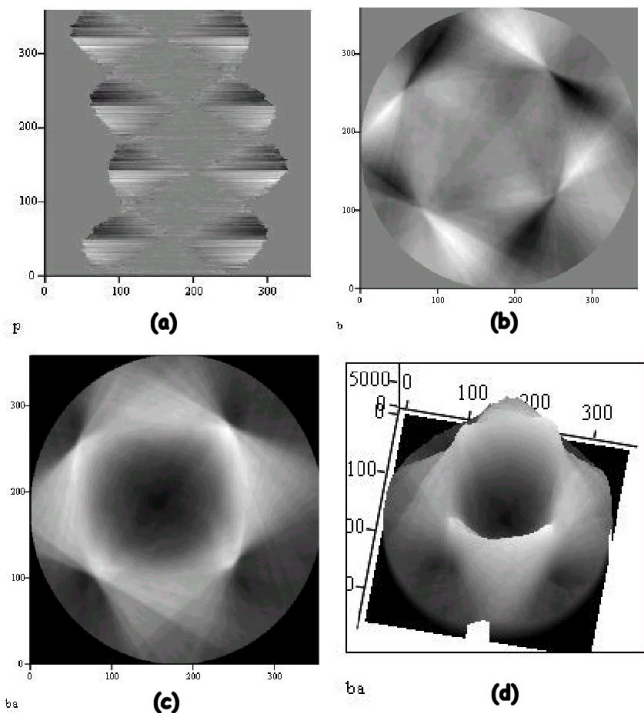


FIGURE 7. Glass squarer bar: (a) Processed experimental sinogram, (b) Reconstruction, (c) and (d) Modulus of reconstruction.

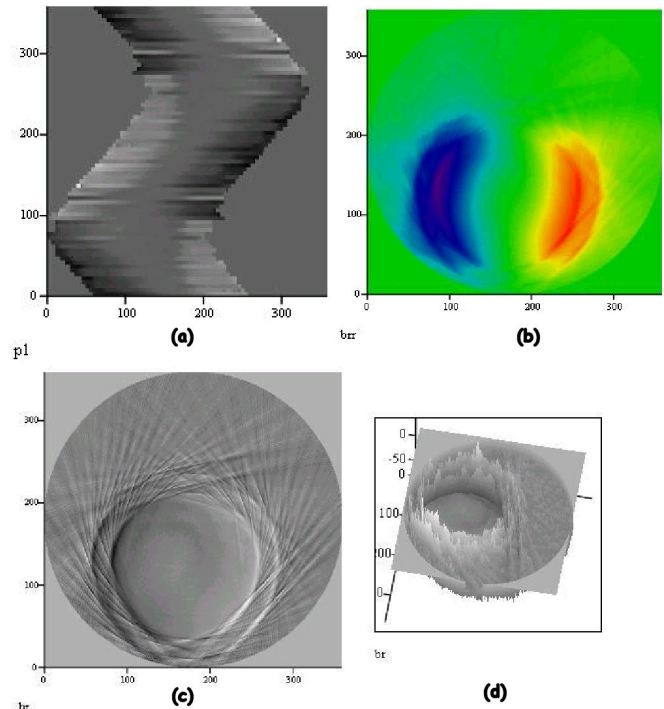


FIGURE 8. Test of glass tube: (a) Processed experimental sinogram, (b) Reconstruction, (c) and (d) Modulus of reconstruction.

5. Conclusions

The proposed method have been probed to be plausible: in particular, parallel projection differences can be extracted with ESPI. Sequential reference derived from the measurement of successive difference of projections offers a wider measurement range with respect to an alternative interferometric method that uses a fixed reference. The sample can be phase-matched with the proper oil immersion within a liquid gate, keeping condition of parallel projections. The same method allows verification of matching condition. Of course, proper fulfillment of matching condition sets limits to the type of objects to be inspected under the method. Although it was used a reconstruction method based on equal stepping angle, other approaches can be more convenient, especially in regions of quick phase changes, thus calling for other algorithm types (algebraic algorithms, for example). Phase unwrapping must be performed in the sinogram plane for the method to reach its full potential. Angular derivative display can render enough information of refractive index distribution so as to get an idea of refractive index distribution. Refractive index distribution recovery remains as a further work, but it can be foreseen that radial derivative data is needed to get enough information.

Acknowledgements

Valuable help and assistance with ESPI (Opto Fringe system v.1.0) from the Optical Metrology Group at Centro de Investi-

gaciones en Optica (Leon, Gto., Mexico) is acknowledged. Support from VIEP-BUAP is greatly appreciated. Partial support from CONACyT (32185) is appreciated.

-
1. G. Rodríguez-Zurita and R. Pastrana Sánchez, *Rev. Mex. Fís.* **43** (1997).
 2. F.J. Ornelas-Rodríguez, G. Rodríguez-Zurita, and R. Rodríguez-Vera, *Optics Communications* **159** (1999).
 3. I.H. Lira and L.E. Moreno, *Meas. Sci. Technol.* **8** (1997).
 4. Stanley R. Deans, *The Radon Transform and Some of Its Applications* (Wiley, New York, 1983).
 5. N. Alcalá-Ochoa, R. Rodríguez-Vera y B. Barrientos, *Rev. Mex. Fís.* **46** (5) (2000).